Chapter 4

Polymer Tandem Solar Cells with Optical Spacer as Interlayer[c]

Abstract

In this Chapter a solution-processed polymer tandem solar cell is described in which the two photoactive single cells are separated by an optical spacer. The use of an optical spacer allows for an independent optimization of both the electronic and optical properties of the tandem cell. The optical transmission window of the bottom cell is optimized to match the optical absorption of the top cell by varying the layer thickness of the optical spacer. The two bulk heterojunction sub cells have complementary absorption maximal at λ_{max} ~ 850 nm for the top cell and λ_{max} ~ 550 nm for the bottom cell. The sub cells are electronically coupled in series or in parallel using four electrical contacts. The series configuration leads to an open-circuit voltage of >1 V, which is equal to the sum of both sub cells. The parallel configuration leads to a high short-circuit current of 92 A/m^2, which is equal to the sum of both sub cells. The parallel configuration results in a higher efficiency compared to the series configuration.

[c] The main results of this Chapter have been published as: A. Hadipour, B. de Boer, and P. W. M. Blom, *J. Appl. Phys.* **2007**, *102*, 074506.

4.1 Introduction

In Chapter 3 a solution-processed organic tandem solar cell was reported that was fabricated from conjugated polymers with complementary absorption spectra and separated by a conducting composite middle contact. In this tandem cell, high energy photons are absorbed in the bottom cell and low energy photons are absorbed in the top cell. In such a stacked geometry, the middle electrode serves two different purposes; as a charge recombination centre, and as a protecting layer for the bottom cell during spin coating of the top cell. The sub cells are electronically coupled together in series, which results in an open-circuit voltage (V_{OC}) of the tandem cell that equals the sum of the V_{OC} of each sub cell. The layer thickness of the bottom cell had to be optimized to in such a way that the optical out coupling is adapted to the absorption of the top cell. A disadvantage of this approach is that the optimum thickness of the bottom cell, required to match the optical output, is not necessarily equal to the thickness where the bottom cell reaches its optimum performance. If, for example, a thickness of 300 nm is required for optical out coupling the occurrence of unbalanced transport may lead to the formation of space-charges, giving rise to a reduced fill factor and performance.[69,38,37] In order to improve the first generation solution-processed tandem cells as described in Chapter 3, we introduce here an additional solution-processable, transparent and insulating layer which serves as an optical spacer and leads to the fabrication of a 4-contact tandem cell. In this second-generation tandem cell, the thickness of the bottom cell is optimized for its electrical performance and the optical out coupling is tuned by varying the thickness of the optical spacer on top of the bottom cell. The transmitted light through the complete stack (bottom solar cell with optical spacer) is matched with the absorption spectrum of the top cell. Since the optical spacer is an insulator, the fabrication of tandem cells with four electrodes is feasible and, consequently, the two sub cells can be coupled electronically (external) in parallel or in series.

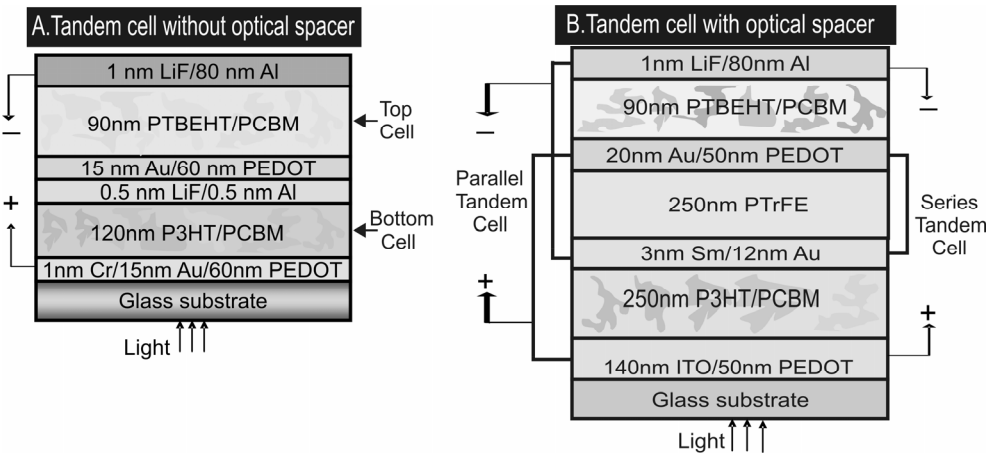

Figure 4.1. A) Schematic structure of the previously mentioned tandem cell in Chapter 3 in which the bottom cell acts as an optical spacer. B) Schematic structure of the second-generation tandem cell in which an additional optical spacer is used that allows for independent tuning of the optical cavity. Two bulk heterojunction cells (bottom and top cell) are stacked in series or parallel outside the device (four terminal devices). The absorption spectra of the two semiconducting polymers P3HT and PTBEHT are complementary.

The optical out coupling and electronic performance of the tandem cells are addressed in the following Sections. The materials and thickness of the electrodes are optimized to have a good optical transmission and a low resistance. Furthermore, the layer thicknesses of both sub cells are optimized for their electronic transport. The bottom cell with the optical spacer processed on top is optimized for its optical transmission in order to harvest the maximum amount of photons on the (infra)red edge of the visible spectrum. Finally, all important parameters are used to design and optimize the 4-electrode tandem solar cell with an imbedded optical spacer.

4.2 Electrodes of the device

The two organic solar cells are linked together by an insulating, solution-processable and transparent layer of poly(trifluoroethylene) (PTrFE) dissolved in methyl ethyl ketone (MEK). This spin coated layer acts as an optical spacer. Due to the presence of the insulating layer of PTrFE the fabrication of the tandem cell now requires four electrodes. The electrodes of the bottom and the top cell can be

connected externally in series or parallel. Consequently, the contacts have to be highly conductive in order to extract and transport the charges from each sub cell. Two of the four contacts used here in the tandem configuration are known to be efficient in BHJ solar cells, namely, 140 nm ITO/50 nm PEDOT:PSS as anode for the bottom cell and 1 nm LiF/80 nm Al as cathode of the top cell. Now, the semi-transparent cathode of the bottom cell and the semi-transparent anode of the top cell have to be defined. The requirements for these electrodes are:

a) as thin as possible to obtain maximum transparency,

b) conductive enough to extract charge carriers,

c) stable during spin coating of the PTrFE optical spacer.

For the cathode of the bottom cell 3 nm of Samarium (Sm) topped with 12 nm Au was found to be very transparent, highly conductive and stable during spin coating of the PTrFE layer. The low work function of Sm (~2.7 eV [82]) provides an Ohmic contact with the bottom cell in order to maximize the open-circuit voltage. The 12 nm Au layer has a sufficiently low resistance for transporting the charge carriers towards the external electrodes. Figure 4.2 demonstrates the difference between two BHJ single cells using ITO/PEDOT:PSS/250 nm P3HT:PCBM (1:1) with different cathodes. Both cells shows the same FF (~64%) and V_{oc} (~0.6 Volt) but the cell with 3 nm Sm/12 nm Au cathode yields a lower photocurrent since this electrode is semi-transparent, resulting in a reduction of the amount of absorbed light. On the other hand, the reflection of a closed layer of 80 nm Al (perfect mirror) is ~ 100 %, which results in a higher photocurrent for a solar cell topped with 80 nm Al.

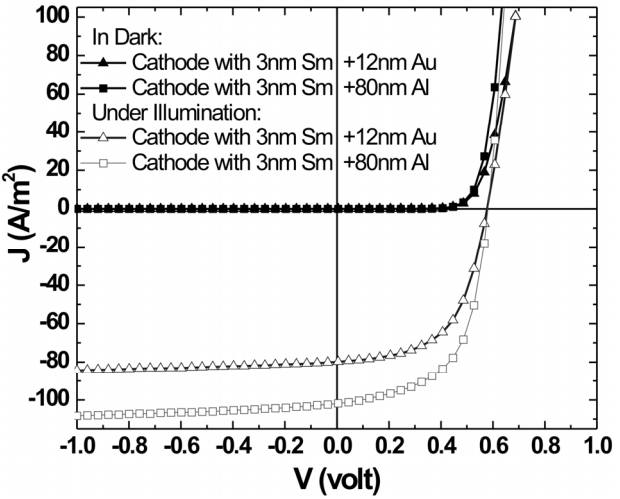

Figure 4.2. Comparison between a semi-transparent cathode made of 3 nm Sm/12 nm Au and a 'perfect' mirror of 1 nm LiF/80 nm Al on top of the bottom cell consisting of a BHJ of 250 nm P3HT:PCBM (1:1). The fill factor and open-circuit voltage of both cells are the same but the photo-generated current of the cell with a semi-transparent cathode is significantly lower.

On top of the PTrFE optical spacer a bilayer of 20 nm Au and 50 nm PEDOT:PSS were chosen for the anode of the top cell. The high and stable work function (~5.2 eV) of PEDOT:PSS forms an Ohmic contact for the top cell to extract the holes. In addition, PEDOT:PSS improves the wetting of the anode for the processing of the top cell. The 20 nm Au layer serves again as conducting layer to extract the holes. This Au layer needed to be optimized for its sheets resistance and optical transparency. To determine its optimal thickness (sheets resistivity versus optical transparency) a reference top cell was fabricated on top of a 250 nm thick layer of PTrFE that was spin coated onto glass substrate. The reference top cell consists of *x* nm Au/50 nm PEDOT:PSS/100 nm MDMO-PPV:PCBM (1:4)/1 nm LiF/80 nm Al as shown in Figure 4.3.

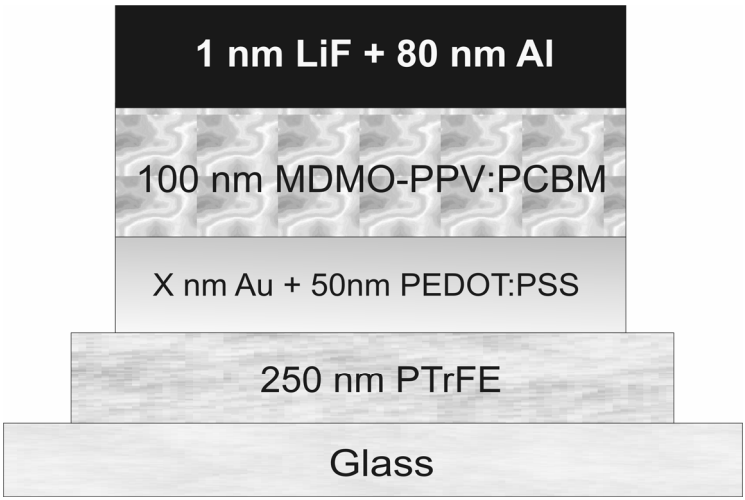

Figure 4.3. The structure of the reference top cell. By varying the thickness of gold (X nm) used in the anode of the device, the thinnest, well-conducting layer can be found.

As Figure 4.4 demonstrates, at least 20 nm Au is needed to create a well-performing device. A thinner layer of Au (15 nm) leads to a very high sheet resistance of the anode and, therefore, to a very poor performance of the cell. This is attributed to the surface roughness of the spin coated optical spacer of PTrFE, leading to the formation of a semi-continuous Au layer.

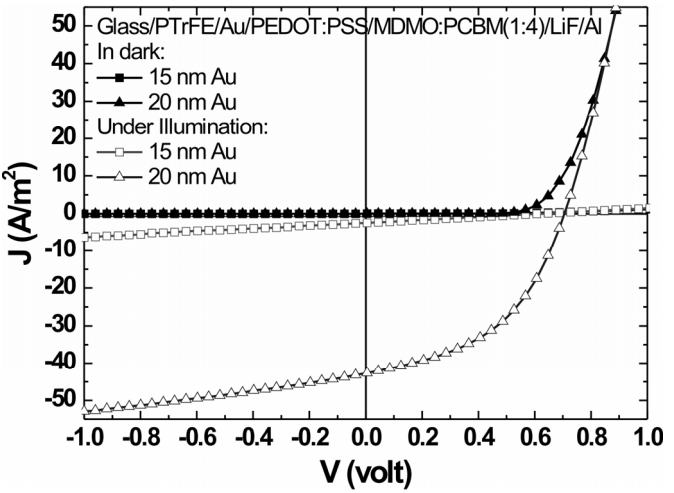

Figure 4.4. Current density–voltage characteristics of a reference top cell structure with different gold thickness at the anode on 250 nm PTrFE. On top of the gold layer a cell is processed based on 50 nm PEDOT:PSS/100 nm MDMO-PPV:PCBM (1:4)/1 nm LiF/80 nm Al. At a thickness of 15 nm the sheet resistance of the contact is too high which leads to a very poor performance of the cell.

The *J–V* performances of two reference top cells are compared in Figure 4.5 with 20 nm and 30 nm thick gold (Au) layers used in the anode of the device. As Figure 4.5 shows, increasing the thickness of the gold layer does not improve the electrical performance of the device.

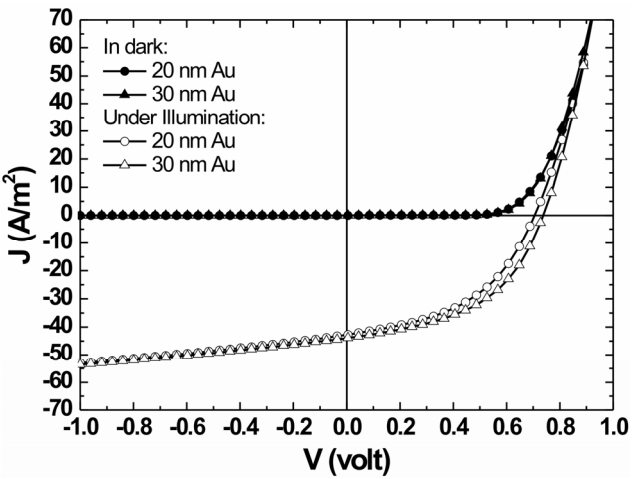

Figure 4.5. Two reference top cells with different anodes are compared. Increasing the thickness of the gold layer used in the anode has little effect on the performance of the device.

Therefore the combination of 20 nm Au + 50 nm PEDOT:PSS was used for the fabrication of the anode of the top cell as most transparent and well-conducting layer.

4.3 Optimum sub cells

Now that we have optimized and defined all anodes and cathodes of the four terminal tandem solar cell, we can further optimize the layer thicknesses of the photoactive layers of the tandem solar cell. These layers can be independently optimized since the optical out coupling of the bottom cell can be tuned by the layer thickness of the PTrFE optical spacer (Figure 4.1). Therefore, blends of P3HT:PCBM (1:1) were spin coated with various layer thicknesses onto the substrates covered with 140 nm ITO/50 nm PEDOT:PSS. The device was topped off with 3 nm Sm/80 nm Al. The structure used for those measurements is shown in Figure 4.6.

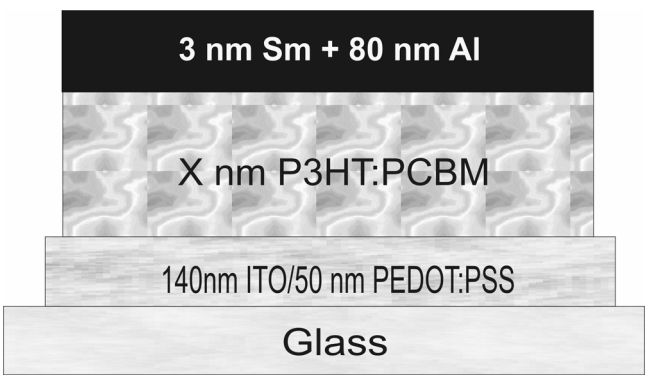

Figure 4.6. Standard device structure for optimizing the bottom cell. By varying the thickness of the active layer, the bottom cell can be optimized for its best electrical performance. Using chloroform as solvent, a 250 nm thick film has the best performance.

The data in Figure 4.7 demonstrate that a cell with a layer thickness of 250 nm of P3HT:PCBM (1:1) performs best. When the active layer is thinner (120 nm, defined by the optical matching of the device in Chapter 3), the amount of absorbed photons is much lower and, consequently, a lower photocurrent is obtained. When

the layer thickness is further increased to 450 nm, the amount of absorbed photons is only slightly increased, but the unbalanced transport of the charge carriers becomes a limitation; The build up of space-charge results in a significant decrease of the fill factor, which in turn leads to a lower total performance.[69]

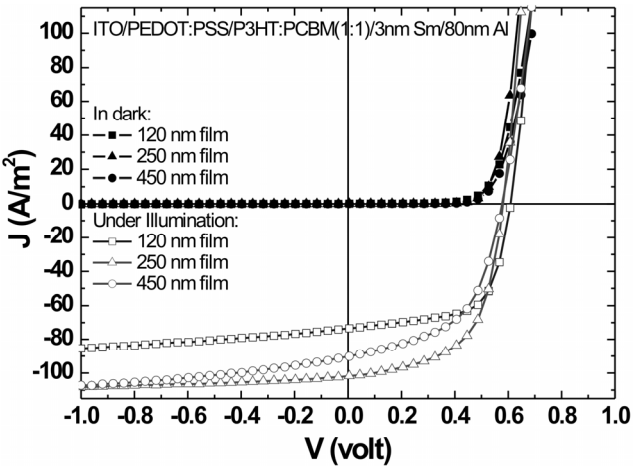

Figure 4.7. Current–voltage characteristics of single BHJ bottom cells with various thicknesses of P3HT:PCBM (1:1). A layer thickness of 250 nm shows the best performance.

By using a standard structure for a single bulk heterojunction solar cell (Figure 4.6), the performance of the top cell can be compared with the performance of the bottom cell. For the top cell we used the conjugated polymer poly{5,7-di-2-thienyl-2,3-bis(3,5-di(2-ethylhexyloxy)phenyl)-thieno[3,4-b]pyrazine} (PTBEHT). The thickness of the top cell made of PTBEHT:PCBM (1:4) was kept to 90 nm, which was found to give the best performance (the chemical structure of PTBEHT is given in Figure 2.1). The *J–V* characteristics of the 250 nm P3HT:PCBM (1:1) and 90 nm PTBEHT:PCBM (1:1) solar cells are plotted in dark and under illumination (1000 W/m^2 , AM1.5) in Figure 4.8.

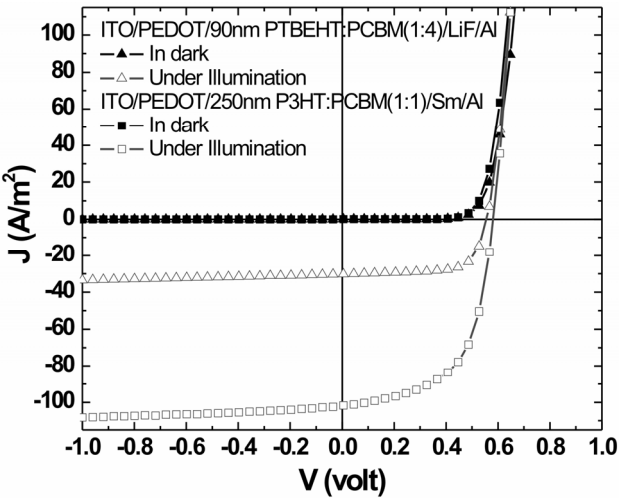

Figure 4.8. The *J–V* characteristic of the active layers used in the bottom (250 nm P3HT:PCBM (1:1)) and top (90 nm PTBEHT:PCBM(1:4)) cells. These reference single cells are measured in dark and under illumination with 1000 W/m^2, AM1.5 solar spectrum.

4.4 Optical considerations

The transparent layer of PTrFE is sandwiched between the semi-transparent cathode of the bottom cell and the semi-transparent anode of the top cell. This allows for the light transmitted through the bottom cell to interfere with the reflected light at the anode of the top cell. Therefore, the thickness of the PTrFE layer affects the total light output through the bottom stack before it reaches the top cell. After optimization of the layer thickness of the bottom cell, the wavelength of the transmitted light output can now be tuned to match the absorption spectrum of the top cell by varying the thickness of the optical spacer (PTrFE layer). The combination of Sm and Au as cathode for the bottom cell is inert for processing of the PTrFE optical spacer, which is spin coated from methyl ethyl ketone (MEK). The advantage of choosing PTrFE is that it can be dissolved in a polar solvent like MEK very fast, but very slowly in solvents like chloroform, chlorobenzene or dichlorobenzene. As a result the solvents used for processing of the active layers of the bottom and the top cell (chloroform or chlorobenzene) are orthogonally compatible with the polar solvent (MEK) used for processing of the optical spacer.

The layer thickness of this transparent PTrFE layer can be easily varied between several tens of nanometers to micrometers. By using donor materials with non-overlapping absorption spectra for the sub cells in a tandem configuration, the utilization of two absorbing polymers with complementary absorption spectrum results in an enhanced photon harvesting of the solar spectrum. Figure 4.9 depicts the normalized absorption spectra of the large band gap polymer P3HT and the small band gap polymer PTBEHT (chemical structure PTBEHT and P3HT inset Figure 4.9) that are used in this study.

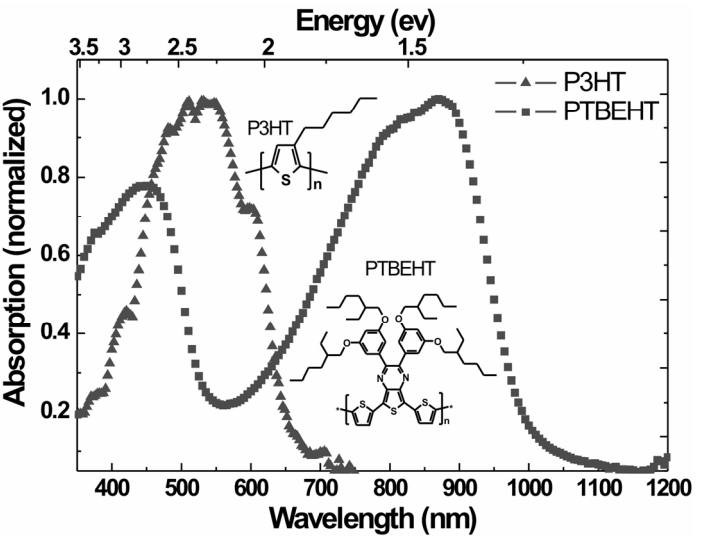

Figure 4.9. Absorption spectra of the large band gap polymer P3HT and of the small band gap polymer PTBEHT with its maximum at 850 nm are shown. The absorption spectra are complementary.

We have performed optical measurements for various layer thicknesses of PTrFE to evaluate the optical transmission of the combined layers. Both the ITO/PEDOT:PSS/P3HT:PCBM/3 nm Sm/12 nm Au stack and the PTrFE sandwiched between 3 nm Sm/12 nm Au and 20 nm Au act as dielectric layers between semi-transparent electrodes. The structure used for the optical measurements is demonstrated in Figure 4.10.

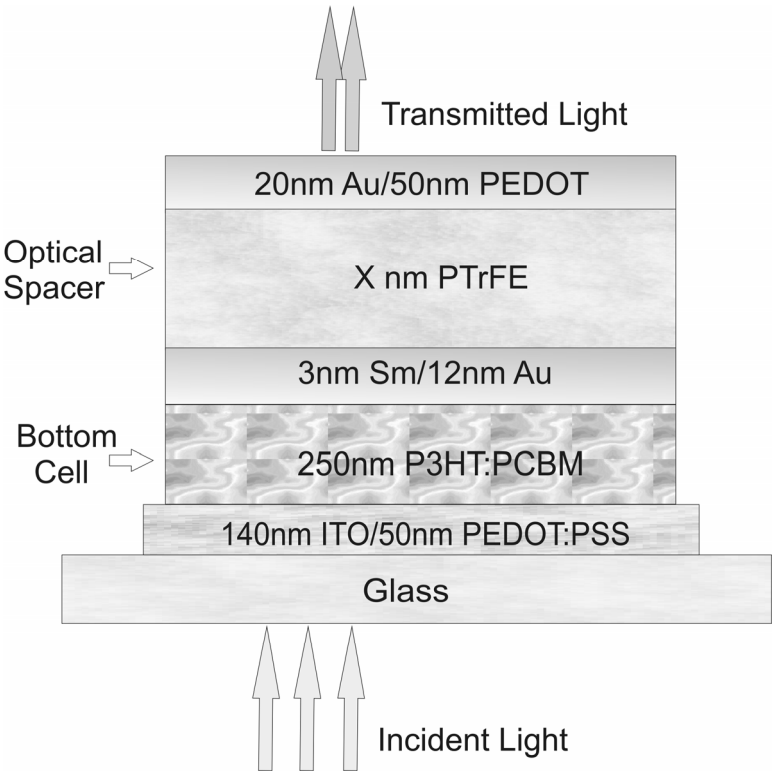

Figure 4.10. Device structure used for the optical matching of the tandem device. The transmitted light through the device has to have the maximum at about 850 nm wavelength where the top cell absorption is maximum..

As demonstrated in Figure 4.11(circles), the transmitted light through the bottom cell consisting of ITO/PEDOT:PSS/250 nm P3HT:PCBM/3 nm Sm/12 nm Au is not yet matched with the absorption spectrum of the top cell. Given the fact that the small band gap polymer (PTBEHT) absorbs between 700 and 950 nm, the optical cavity (or layer thickness) of the optical spacer has to be optimized in order to transmit in this wavelength range. Figure 4.11 (triangles) demonstrates that a layer thickness of the optical spacer of 250 nm, in combination with 250 nm P3HT:PCBM/3 nm Sm/12 nm Au, results in an optical out coupling of the bottom stack that matches the absorption of the small band gap polymer in the top cell. The bottom cell processed from 250 nm P3HT:PCBM (1:1) topped with an optical

spacer (PTrFE) of 250 nm transmits about 50 % in the wavelength range that is absorbed by the small band gap polymer PTBEHT (Figure 4.11 dotted line).

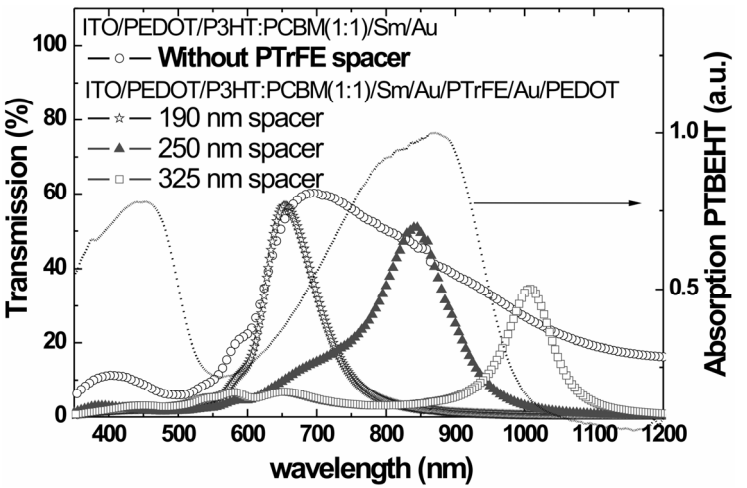

Figure 4.11. Transmission of incident light through the bottom cell consisting of glass/140 nm ITO/50 nm PEDOT:PSS/250 nm P3HT:PCBM (1:1)/3 nm Sm/12 nm Au/*x* nm PTrFE/20 nm Au/PEDOT:PSS. For a blend of P3HT:PCBM (1:1) with a layer thickness of 250 nm (and no optical spacer), the light output is not yet matched with the absorption of the top cell (700–950 nm, spectrum given by the dotted line). By spin coating an additional transparent layer of PTrFE, the transmitted light can be tuned in order to match the absorption of the top cell.

4.5 Electrical considerations

In this second-generation tandem geometry, the bottom and the top cells can be electronically coupled either in series or in parallel. When the bottom and top cells are connected in series, the open-circuit voltage (V_{OC}) of the tandem cell is equal to the sum of the open-circuit voltages of both individual cells. The photocurrent density of the tandem cell becomes limited by the lowest photocurrent density of the two sub cells (the top cell in Chapter 3). As shown from the single reference cells (Figure 4.8) the cells based on PTBEHT generate less photocurrent as compared to the P3HT based cells. Combined with the fact that the top cell is also illuminated with lower light intensity (~50%), the photocurrent of the top cell is substantially lower as compared to the bottom cell. The *J*–*V* measurements of the individual bottom and top cells, and of the tandem cell connected in series are depicted in Figure 4.12A. As expected, the top cell strongly limits the photocurrent of the tandem cell. In this four terminal tandem geometry, the two sub cells can

also be easily connected in parallel. Since both cells produce the same V_{OC} the tandem solar cell connected parallel is expected to have the same V_{OC} as both sub cells (no losses). In contrast, the current that can be extracted from the parallel tandem cell is now the sum of the photocurrent of the bottom and top cell. This implies that the lower current of the top cell does not limit the tandem cell in parallel configuration. The current density–voltage characteristics for the bottom, top and the parallel tandem cell are plotted in Figure 4.12B. Since the top cell generates a much lower photocurrent as compared to the bottom cell the parallel tandem solar cell leads to a higher performance as compared to the tandem solar cell connected in series. Indeed, the open-circuit voltage of the parallel tandem cell (0.59 Volt) is close to the V_{OC} of the bottom (0.60 Volt) and top cells (0.51 Volt), while the current is the sum of both photocurrents generated by the two sub cells. A direct comparison between the series and parallel configuration is shown in Figure 4.12C; the series configuration has a high open circuit voltage (V_{OC} = 1.03 V), while its short circuit current (J_{SC} = 16.3 A/m^2) is limited by the lower current of the top cell. The parallel configuration shows the same open circuit voltage as both sub cells (V_{OC} = 0.59 V), combined with a high short circuit current (J_{SC} = 92.0 A/m^2). The values of the V_{OC}, J_{SC}, FF and efficiencies of the bottom, top, series tandem and parallel tandem solar cells are summarized in Table 4.1. The performance of the parallel tandem cell is much better than the series tandem cell where the photocurrent is limited by the low photocurrent of the top cell. However, it should be noted that in the present parallel configuration the performance hardly exceeds the performance of the bottom cell alone (estimated efficiency is 3% for both bottom and parallel tandem cell). Since the current of this tandem cell is equal to the sum of the currents generated by both sub cells, the lower fill factor (FF) of the top cell (50%) (Compared to the high FF of the bottom cell (64%)) also affects the fill factor of the tandem cell (54%). This lower fill factor compensates the gain in photocurrent in the parallel tandem solar cell. In the case of two sub cells having similar fill factors, the parallel configuration will always results in a tandem solar cell with higher performance as compared to the individual sub cells.

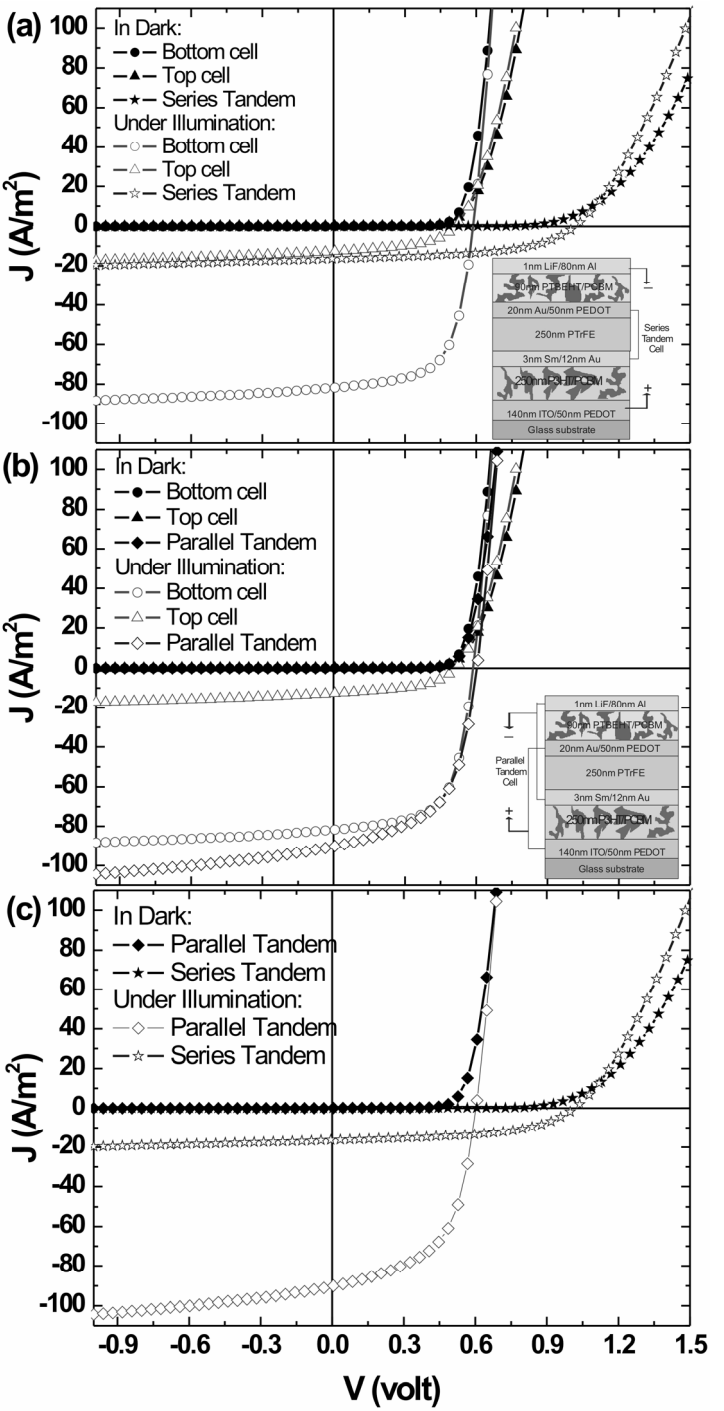

Figure 4.12. A) *J–V* characteristics of the bottom and top cell measured separately, and the tandem cells connected in series in dark and under illumination with 1000 W/m^2, AM1.5. The current density is limited by the lowest current density of the two cells and the open-circuit voltage is the sum of both sub

cells. B) *J–V* characteristics of the bottom and top cell measured separately, and the tandem cells connected parallel in dark and under illumination with 1000 W/m^2, AM1.5. The current density is equal to the sum of both sub cells and the open-circuit voltage is limited to the lowest V_{OC} of the sub cells. C) The *J–V* characteristics of the series tandem cell versus the parallel tandem cell.

Solar cell type	V_{OC} (V)	J_{SC} (A/m^2)	FF (%)	η (%)
Bottom cell	0.60	81.6	64	~3
Top cell	0.51	12.7	50	~0.31
Series Tandem cell	1.03	16.3	51	~ 0.85
Parallel Tandem cell	0.59	92.0	55	~3

Table 4.1. The quantitative values extracted from the *J–V* measurements of the individual and tandem photovoltaic cells. Illumination conditions: 1000 W/m^2, AM1.5.

4.6 Device fabrication

The devices were fabricated on cleaned glass/ITO substrates. A 50 nm thick poly(3,4-ethylene dioxythiophene) : polystryrenesulfonic acid (PEDOT:PSS, H. C. Starck) was spin coated and dried in an oven at 140 °C for 15 minutes. The bottom cells were based on blends in a 1:1 ratio of regioregular poly(3-hexylthiophene) (P3HT, see Figure 6)) and the fullerene derivative [6,6]-phenyl-C_{61}-butyric acid methyl ester (PCBM) processed from chloroform. The P3HT:PCBM film was annealed at 135 °C for 2 hrs using a hot plate in the glove box under nitrogen atmosphere. The top cell was processed from a $CHCl_3$ solution of the poly(di-2-thienylthienopyrazine) derivative PTBEHT (see inset Figure 6) and PCBM in a 1:4 ratio. Poly{5,7-di-2-thienyl-2,3-bis(3,5-di(2-ethylhexyloxy)phenyl)-thieno[3,4-b]pyrazine} (PTBEHT) was synthesized from the corresponding dibrominated monomer via a condensation polymerization using bis(1,5-cyclooctadiene)nickel(0) [$Ni(COD)_2$].[24] PTBEHT was extensively purified by removing Ni with EDTA

disodium salt, Soxhlet extraction using different solvents, and finally a BioBeads GPC column to remove the low molecular weight fraction. The molecular weights as determined with size exclusion chromatography are M_n = 52,000 and M_w = 160,000 (PDI =3.1). PTBEHT is soluble in most common organic solvents. The optical spacer was fabricated from poly(trifluoroethylene) (PTrFE) dissolved in methyl ethyl ketone (MEK). The spin coating of the PTrFE was done with high rpm's for increasing the flatness of the layer. All conjugated polymers and PCBM were dissolved in chloroform and mixed in the designated weight ratio. A proper spin program was chosen to tune the thickness of the layers (250 nm for P3HT:PCBM and 90 nm for PTBEHT:PCBM). For the cathode of the bottom cell, using a shadow mask, 3 nm Sm and 12 nm Au were vapor deposited (at 10^{-7} mbar). The deposition-rate of the Sm has to be very slow (~ 0.01 nm/sec) for creation as small as possible island of the Sm-interlayer. The Au layer has to be deposited with high rate (~ 0.5 nm/sec) in order to increase the size of the islands of gold during evaporation process. This leads to lower penetration depth of the Au atoms into the polymer surface and sharper interface and therefore higher performance of the bottom cell. PTrFE was dissolved in MEK and spin-coated onto the bottom cell in various layer thicknesses. On top of the PTrFE layer, using a shadow mask, 20 nm Au was evaporated and 50 nm PEDOT:PSS was spin coated. Here, the gold has to be evaporated with high evaporation-rate (~ 0.5 nm/sec) for the same reasons as before. The complete stack was dried in a vacuum chamber at 10^{-2} mbar (1 Pa) for 30 minutes in order to evaporate the water in the PEDOT:PSS. For the active layer of the top cell, the polymer PTBEHT as electron donor and PCBM as acceptor were used in a 1:4 ratio. Both were dissolved in chloroform. A proper spin program was chosen to tune the thickness of the layers (90 nm PTBEHT:PCBM (1:4) film). For the top contact, using a shadow mask, 1 nm LiF and 80 nm aluminum (Al) were thermally evaporated. The thicknesses of the different layers were measured by a Dektak 6M profilometer. All optical measurements were performed on a Perkin–Elmer Lamda 900 Spectrometer. The *J*–*V* measurements (in dark and illuminated) were done by using a Keithley 2400 source meter. The illumination was done using a AM1.5 simulated solar spectrum from a Steuernagel Solar Constant 1200 light source with an intensity of 1000 W/m^2. The processing was done in a glove box under nitrogen and at room temperature.

4.7 Summary

Solution-processed organic tandem solar cells were fabricated using an electrically insulating and solution-processable optical spacer. The optical spacer is based on the transparent poly(trifluoro ethylene), which is spin coated from a MEK solution. This polar solvent is orthogonally compatible with the solvents of the active layers of the solar cells and leaves the bottom cell unaffected. By varying the thickness of the optical spacer, the transmission through the bottom cell and spacer is tuned to match the absorption of the top cell. This allows for an independent optimization of the thickness of the bottom cell for its best electrical performance. Furthermore, the tandem solar cell can electrically address in series or parallel. The performance of the series tandem solar cell is limited by the low current of the top cell, even though the V_{OC} is equal the sum of both sub cells and amounts to > 1 V. The parallel tandem cell has a much higher efficiency since the V_{OC} of the parallel tandem cell is equal to the V_{OC} of both sub cells and the photocurrent density is equal to the sum of the photocurrent densities of both sub cells. The lower FF of the top cell limits the performance of the parallel tandem cell.